39th Joint Propulsion Conference AIAA 2003-5165
Huntsville Alabama, 21-24 July 2003

EXPERIMENTAL EVALUATION OF SUB-SCALE CBIO ION OPTICS SYSTEMS

D. Mark Laufer,[*], John D. Williams,[‡] Casey C. Farnell,[*]
Paul B. Shoemaker,[†] and Paul J. Wilbur[§]
Colorado State University
Fort Collins, CO 80523

ABSTRACT

An experimental study of a sub-scale **c**arbon-**b**ased **i**on **o**ptics (CBIO) design proposed by the Jet Propulsion Laboratory (JPL) is described. Perveance and crossover beamlet current limits, above and below which accelerator grid direct impingement currents rise, are documented over wide throttling ranges. Test data reported for assemblies with 1, 7, 19, and 37 aperture pairs suggest that gridlets containing only a small fraction of the total number of apertures in a full-sized optics system can be used to investigate the behavior of larger systems. A study of the effects of grid spacing on beamlet current-limit data that was performed using different types of mica spacers is also presented. Comparisons to numerical simulations suggest that the mica spacer that contained organic binder material changed dimensions slightly during testing. The second type of iso-mica, which is intended for high temperature service, was much more stable and better suited to the hotter test conditions that occur during operation at high specific impulse. In addition, results are presented that examine the onset of the electron backstreaming condition that can develop at the end of life (EOL) in some mission scenarios. Backstreaming voltage limits were measured for grid spacings that simulate their transient behavior and for accel holes with progressively larger accel diameters that simulate the effects of accel barrel erosion over life.

INTRODUCTION

The beamlet current range over which a particular ion optics system can be operated is generally limited by the onset of destructive direct ion impingement at both high and low beamlet current values. These limitations can manifest themselves during initial testing of a grid set or after many tens of thousands of hours of operation during a particular mission or acceptance/qualification test sequence, especially when wide throttling ranges are involved.

When the beamlet current is low, the sheath that separates the discharge chamber plasma from the ion acceleration region is dished upstream to the point where ions are over-focused, their trajectories cross, and, at the limit, ions in the beamlet begin to impinge directly on the downstream edge of the accel grid barrel. When the beamlet current is high, on the other hand, the sheath is dished less, and the ions can be under-focused to the point where they begin to impinge directly on the upstream side of the accel grid. These behaviors define the crossover and perveance limits on beamlets that are extracted over the full diameter of a given ion optics system.[1,2] Careful attention must be paid to these limits to prevent direct ion impingement and rapid accel grid erosion.[3]

A third and equally important operational limit on ion optics systems is the backstreaming limit, which is the voltage magnitude that must be applied to the accelerator grid to prevent beam plasma electrons from backstreaming. Ideally the accel grid voltage should be held negative of but as close to this limit as possible. This will ensure that damage due to the small current of charge exchange ions that sputter erode and limit the lifetime of this grid will be minimized. Unfortunately, the backstreaming limit can change as the accel grid wears over time, and compromises on selecting the magnitude of the accel voltage must be made. Many factors can affect the backstreaming voltage including aperture geometry and beamlet current. The plasma flow field environment in the ion beam is also an important factor in determining the backstreaming limit.[4] The onset of backstreaming can also be strongly affected by the operational conditions associated with the neutralizer and conductive plasma-bridge that forms between the neutralizer plasma and the beam plasma.[1]

In this paper, we describe the experimental apparatus and procedures used to conduct tests on CBIO[5] gridlets. Next, test results are presented for both beamlet current and backstreaming limitations of CBIO gridlets fabricated with 1 to 37 apertures. This study was performed to determine the minimum number of apertures required to simulate an actual ion optics system accurately. Additional test data are presented for experiments where the grid separation distance

*Graduate Research Assistant, Member AIAA
†Undergraduate Laboratory Assistant, Member AIAA
‡Assistant Professor, Senior Member AIAA
§Professor, Senior Member AIAA

and accel hole diameter were varied and tested over a wide range of specific impulse. These results are used to describe effects of (1) thermal transients that occur at startup that may cause grid gaps to vary, (2) variations in grid gap that will occur due to manufacturing and grid assembly tolerances, and (3) barrel erosion that can occur over the lifetime of the ion optics system. We compare beamlet current limitation and electron backstreaming measurements to analytical and numerical calculations, and areas of disagreement between the experiments and modeling results are used to motivate discussions of additional experimentation that is needed. Finally, conclusions are presented along with recommendations for future work.

APPARATUS AND PROCEDURES

A sketch of the gridlet test facility is shown in Fig. 1. Tests were conducted by mounting a two-grid, 1 to 37 aperture pair assembly to a ring-cusp discharge chamber. The grids were fabricated from Poco graphite using a computer controlled milling center. The screen and accel gridlets were insulated from one another using two different types of iso-mica sheets and were aligned through the use of precision-placed alignment holes. One of the iso-mica spacers used organic binder materials, and the second used an inorganic binder material. During the manufacturing process, the inorganic mica spacers were fired to 650 °C. All mica spacers used in this study were obtained from Von Roll Isola Inc., Midwest Mica Division, Cleveland Ohio.

The beam voltage applied to the screen grid and boosted by the discharge chamber anode power supply (not shown in Fig. 1) was measured relative to tank ground. It is noted that the inner diameter of the discharge chamber anode is 15 cm and this was quite a bit larger than the active diameter of the gridlets tested (~1 cm). This was done to ensure that the discharge chamber plasma properties would be uniform over the entire gridlet area, and thereby impose common behavior in all beamlets to allow division of the measured beam current (J_B) by the number of apertures to obtain the beamlet current (J_b). A ground screen was placed between most of the inactive area of the accel grid and the beam plasma to limit the collection of beam plasma ions on the accel grid surface. The impingement current collected by the accel grid was measured using the ammeter shown in Fig. 1 (labeled J_A) and converted to a per beamlet value by dividing its reading by the number of accel grid apertures.

The ion beam was neutralized using a remotely located plasma source. It consisted of a 6-cm diameter, ionization stage that was equipped with a hot filament cathode. The neutralizer plasma probe has been operated over a wide parameter space of flow rate, discharge power, and coupling bias in a previous study to investigate the effects these parameters had on gridlet performance and results of these tests are documented in Ref. 1. For all of the electron backstreaming characterization testing performed in this study, the neutralizer discharge power was set to 3 W, the neutralizer flow rate to ~0.4 sccm, and the coupling voltage to -15 V based on results obtained from this earlier study.

The vacuum test facility was ~41 cm in diameter and was pumped by a diffusion pump equipped with a water-cooled baffle. The base pressure was in the low 10^{-6} Torr range after baking the vacuum chamber for 1 to 2 hours. Xenon flow rates from ~30 to 150 mAeq induced pressures of $2x10^{-5}$ to $3x10^{-4}$ Torr. It is noted that larger vacuum facilities are available in our laboratory that would enable gridlet operation in the high 10^{-7} Torr pressure range. One such facility is also equipped with a 0.9 m diameter diffusion pump and a refrigeration-cooled baffle (-70 °C).

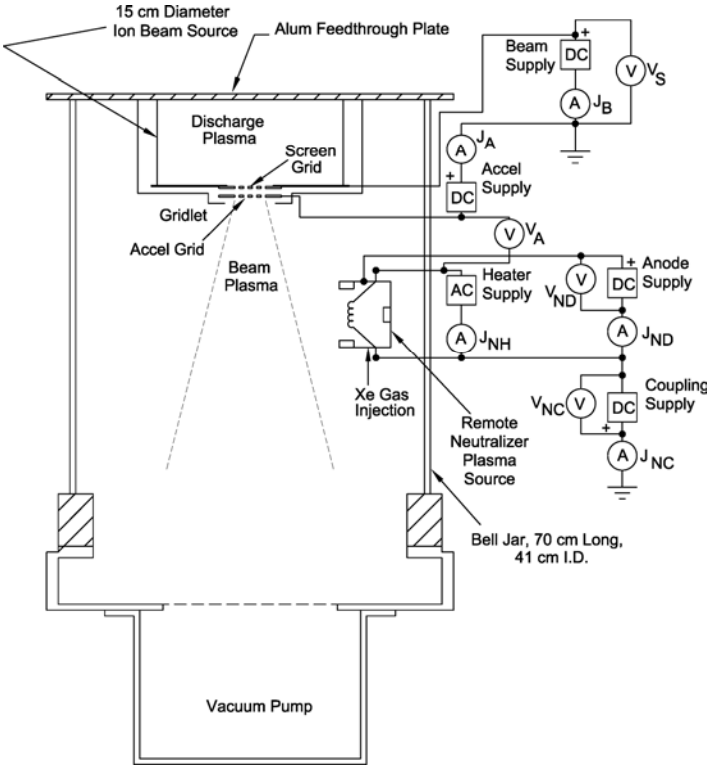

Fig. 1 Sketch of test apparatus showing gridlet ion source and neutralizer layout and wiring diagrams.

Gridlet testing involves measurement of the beam and accel current as the ion source discharge chamber power is varied. We fixed the discharge voltage to 30 V for all of the tests reported in this paper. The flow rate was also fixed at the start of a particular test to a value that was slightly larger than that required to operate at the perveance limit of the gridlet under test. Propellant utilization efficiencies at the perveance limit condition were typically between 50 and 75%. The gridlet tests were performed over wide ranges of both beam

voltage and accel voltage to obtain throttling behavior and backstreaming data.

Figure 2 contains a sketch of the gridlet geometry and the corresponding nomenclature that will be referred to in this paper. As mentioned in the introduction, we have focused on testing of gridlets fabricated to the CBIO geometry, and the dimensions of these gridlets are listed in Table 1. In addition to the nominal grid dimensions, Table 1 contains beam and accel voltages and corresponding specific impulses where experimental data were collected.

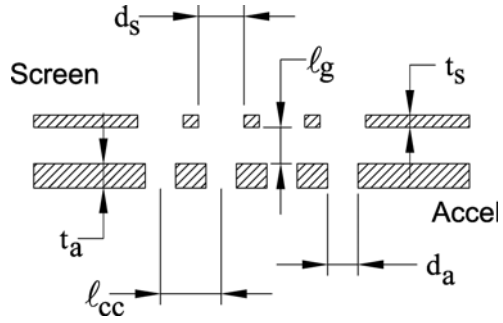

Fig. 2 Gridlet geometry definitions.

TABLE 1 CBIO grid geometry and throttling conditions.

	Symbol	Value*	Description
Geometry	d_s	1.21	Screen hole diameter
	t_s	1.21	Screen grid thickness
	ℓ_g	1.21	Gap between screen and accel grids (nominal)
	d_a	1.21	Accel hole diameter (BOL)
	ta	2	Accel grid thickness
	ℓ_{cc}	1.21	Hole center-to-center distance
Operating Conditions	I_{sp}	4050 s	Specific Impulse (nominal with xenon propellant)
	V_b	1800	Net accelerating voltage (nominal beam voltage)
	V_a	-190	Accel voltage (nominal)

* Multiplication factor relative to similar dimension of NSTAR ion optics system.

Throttling Conditions:

I_{sp} = 2700 s V_b = 800 V V_a = -140 V	I_{sp} = 3600 s V_b = 1420 V V_a = -170 V	I_{sp} = 4050 s V_b = 1800 V V_a = -190 V
	I_{sp} = 4500 s V_b = 2220 V V_a = -200 V	

RESULTS

The results of this study are presented in two sections. The first section focuses on presentation of the experimental results as the beamlet current, beam voltage, accel voltage, and gridlet geometry were varied in a systematic manner. The second section presents comparisons between the experimental results and numerical simulations performed using the igx code.

Experimental Measurement of Ion Optics Limits

Typical accel grid impingement current data display a "U" shape when plotted as a ratio of impingement-to-beamlet current versus beamlet current as shown in Fig. 3. Note that the beamlet current was varied in this experiment by varying the discharge current while holding the discharge, beam, and accel voltages constant. At low beamlet currents, the relative impingement current rises due to crossover ion impingement on the downstream edge of the accel hole barrels. At moderate beamlet currents, the relative impingement current is flat and at a value dependent upon the background neutral density and the propellant utilization efficiency of the ion source. In our small vacuum facility operating at low propellant utilization, the relative impingement current typically lies between 1 and 10% of the beam current. As the beamlet current is increased to higher values, the relative impingement current will again rise quickly indicating that direct ion interception is occurring on the upstream edge of the accel hole barrels due to perveance (or space-charge) limitations. Figure 3 indicates that the safe operating range of the CBIO grids is relatively large and the ratio of perveance to crossover beamlet currents is ~6. The data presented in Fig. 3 were collected with two independent sets of screen gridlets that were mated to the same accel gridlet before testing. The agreement between the data sets indicates that our fabrication and assembly techniques are adequate for performing impingement limit testing.

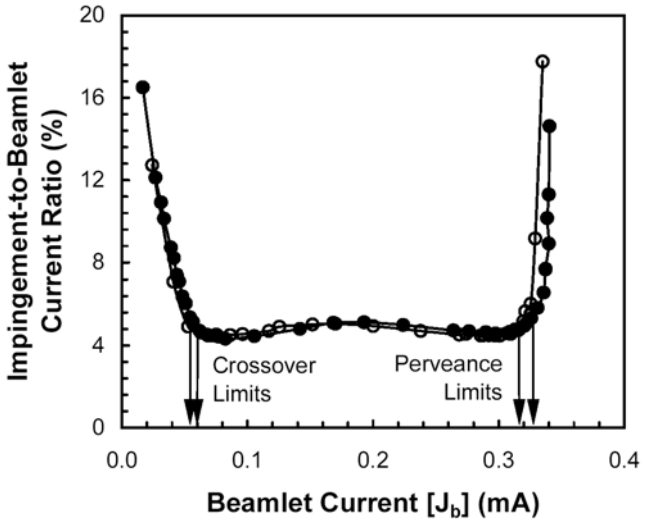

Fig. 3 Typical impingement current behavior for identical 37-hole CBIO gridlets operated at a specific impulse of 4050 s (ℓ_g ~ 30% greater than nominal value listed in Table 1).

A basic assumption of gridlet testing is that experimental measurements made using a small number of ion-extraction holes exposed to a uniform discharge chamber plasma will exhibit the same optical behavior as a typical hole in a full-sized grid set that sees the same plasma conditions. It is recognized, however, that holes around the gridlet periphery will be only partially surrounded by other holes and that the sheath boundary and hence the ion beamlet focusing will be slightly different between the regions around a hole where there are and are not adjacent holes. The effects should be greatest at low beamlet currents where the sheath that separates the discharge chamber plasma from the ion acceleration region is dished and offset upstream from the screen hole to the point where sheaths from adjacent holes can interact. There is experimental evidence[6] from high specific impulse gridlet testing of larger sized gridlets that sheath shapes influence beamlet focusing and that operational limits are influenced by the fraction of a hole circumference that is in contact with adjacent holes. The adjacent sheath effect has been found to be especially significant for large screen hole aspect ratios (d_s/t_s=14) in large gridlets,[5] however, smaller aspect ratios of d_s/t_s=4.7 were shown to be less problematic. It is noted that the CBIO screen hole aspect ratio is equal to five.

In order to determine the number of holes that are completely and partially surrounded by other holes consider the following sketch of a 60° segment of a hexagonal hole layout pattern.

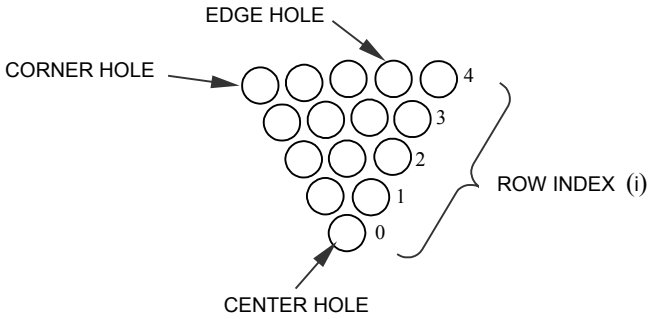

Fig. 4 Pie shaped section of a gridlet hole layout pattern showing surrounded holes, edge holes, and corner holes.

The number of holes in a full (360°) hexagonal pattern obtained via five-fold rotation of the pattern about the center hole can be expressed in terms of the final or outer-row index (n) by the equation

$$h(n) = 1 + 6\sum_{i=0}^{n} i \quad . \qquad (1)$$

The extent to which holes are affected by other adjacent holes is determined by recognizing that all holes with the exception of the outer row are completely surrounded and that the outer row has some adjacent holes. For corner and edge holes shown in Fig. 4, the partial adjacency amounts to 1/3 and 1/2 respectively, of the maximum of six surrounding holes for the hexagonal pattern. Hence the number of holes that are effectively surrounded for an outer row n is given by the expression

$$e(n) = h(n-1) + 6\left[\frac{1}{3}\right] + 6\left[\frac{n-1}{2}\right] = h(n-1) + 2 + 3(n-1) \quad . \qquad (2)$$

The ratio e(n)/h(n) is the fraction of the accumulated circumference of all the holes that are bounded by adjacent-hole interactions. This ratio is plotted against the number of gridlet holes determined from Eq. 1 in Fig. 5. It shows that the fraction, which is obviously zero for a single hole, rises rapidly to 43% and then 63% for 7 and 19 holes (corresponding to n = 1 and 2), respectively.

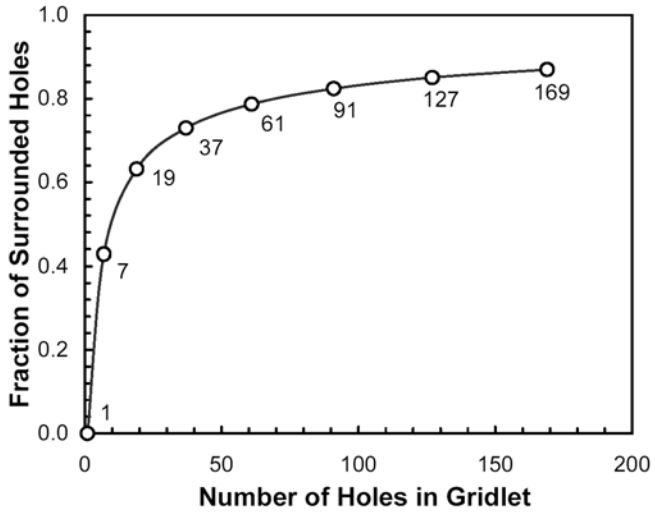

Fig. 5 Fraction of holes surrounded by adjacent holes as a function of hole number.

Perveance and crossover beamlet current limits like the ones identified in Fig. 3 were determined for gridlets with 1, 7, 19, and 37 holes (or apertures), and results are plotted in Fig. 6. The important result of these tests is that both the perveance and crossover limits remain relatively unchanged for the CBIO geometry as the number of holes was varied. From results presented in Figs. 5 and 6 and because sheath shape influences due to non-adjacent holes can be expected to be of second order, we conclude that it should indeed be possible to represent the performance of a full grid set using data obtained from tests conducted with gridlets having a relatively small number of holes.

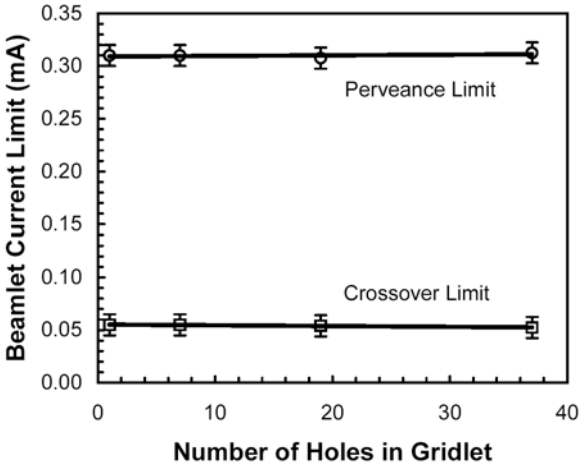

Fig. 6 Perveance and crossover beamlet current limits measured as a function of the number of aperture sets at a specific impulse condition of 4050s.

Figure 7 shows accel grid impingement current data that were collected over the range of net accelerating voltages listed in Table 1. The data indicate the expected increase in perveance limit as the net and total accelerating voltages were increased. In addition, the crossover limits were observed to increase as the net and total accelerating voltages were increased. It is noted that a different insulating spacer was used between the data sets shown in Figs. 6 and 7. This change was necessary because the gridlet temperature was higher at the 4500-sec condition and the original, organic binder-based iso-mica insulators were charring. The new insulators were made from the inorganic binder-based, high temperature-stable mica paper. The data contained in Fig. 7 correspond to the nominal gridlet spacing listed in Table 1.

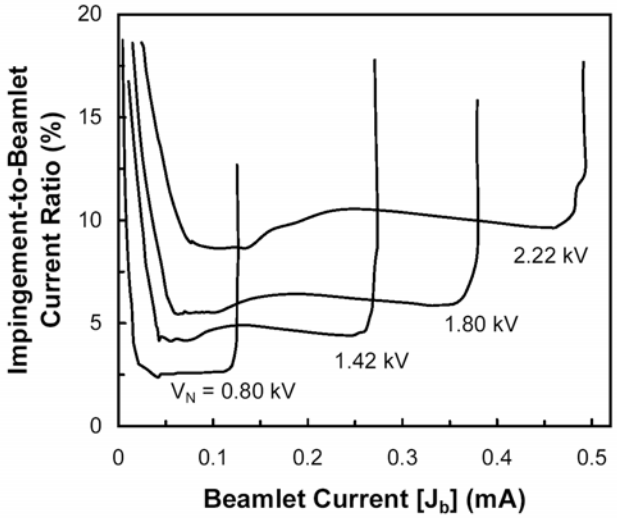

Fig. 7 Perveance and crossover limit behavior as a function of throttling condition (see Table 1).

Many data sets like the ones shown in Fig. 7 were obtained at different accel hole diameter and grid spacing conditions. Perveance limits taken from these data sets are plotted in Figs. 8a and 8b as functions of the net accelerating voltage. (See Table 1 for corresponding total voltage and specific impulse levels.) The larger than nominal accel hole diameters were chosen in this study to correspond to 29 and 61% increases in accel hole area, and the largest accel hole corresponds to a diameter midway between the BOL accel hole diameter and the screen hole diameter. Figure 8a shows that the perveance limit increased slightly when the accel diameter was increased to 14% above nominal. The limit increased more when the diameter was increased to 27% above nominal. It is interesting to note that the perveance limit measured at the 4050 sec condition increased by only 16% when the accel hole area was increased by 60%. The relatively mild effect of accel hole area on perveance limit was expected from results of previous measurements made with larger gridlets operated at higher specific impulse.[5] It is noted that the data contained in Fig. 8a were collected with organic-based iso-mica spacers, and the perveance limits at the nominal gridlet spacing and accel diameter were observed to fall slightly below values obtained with inorganic-based iso-mica spacers as indicated in Fig. 7.

Figure 8b contains perveance limit data collected at two grid spacing conditions that were smaller (-6% and –20%) and one larger (18%) than the nominal grid spacing. As expected from Child-Langmuir law considerations, the larger grid spacing corresponds to lower perveance limits and the smaller grid spacings correspond to higher perveance limits.

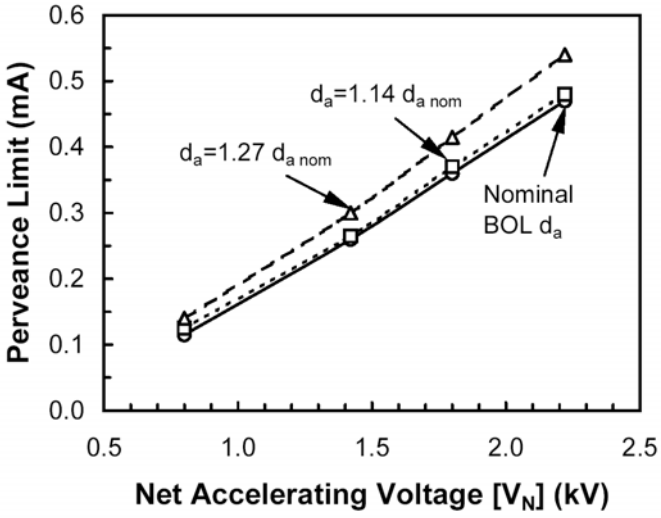

Fig. 8a Perveance limit behavior as a function of accel hole diameter.

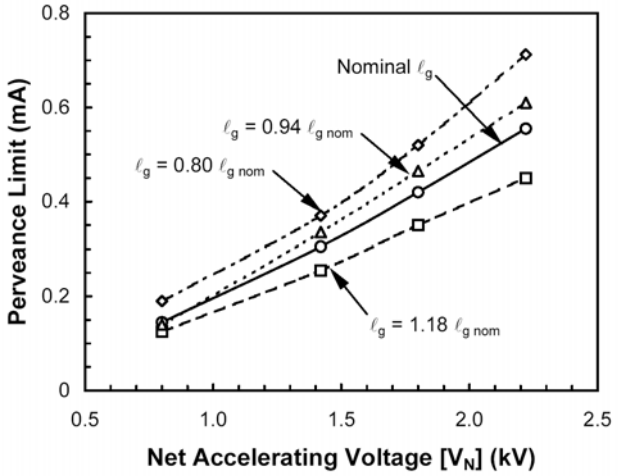

Fig. 8b Perveance limit behavior as a function of grid spacing.

The ability of an ion optics system to impart a negative potential throughout the beamlet volume near the axial location of the accel grid determines its capacity to stop beam plasma electrons from backstreaming into the discharge chamber. The geometry of a typical ion optics aperture set applies boundary conditions that result in an electrostatic potential saddle point being formed near the axial location of the accel grid on the beamlet centerline. The saddle point presents the lowest resistance path to electrons on trajectories that could carry them from the beam plasma toward the discharge plasma.[4] The magnitude of the negative voltage that must be applied to the accelerator grid to prevent electron backstreaming, the backstreaming limit, was measured at each beamlet current and grid geometry condition investigated. Two typical curves showing the sudden increase in apparent beamlet current that occurs at the backstreaming limit are displayed in Fig. 9. The ordinate in this plot is the ratio of beamlet currents measured at $|V_a|$ and at a voltage significantly greater than the backstreaming limit, namely $|V_a|$ = 190 V. At the backstreaming limit, electrons drawn upstream from the beam plasma into the discharge chamber plasma cause the increase in apparent beamlet current.

Figure 9 contains a total of four curves that were recorded at two different beamlet current values. The solid symbols correspond to one 37-hole gridlet set, and the open symbols correspond to a separate, but identical set. Higher accel voltage magnitudes were required to stop electrons from backstreaming through the gridlets when they were operated at moderate beamlet current values. To investigate this further, a test was performed where backstreaming data were collected over the entire beamlet current range from the crossover to perveance limits. The backstreaming voltage limits determined from this test are plotted in Fig. 10. The point where backstreaming is most likely to occur was observed to be at a beamlet current that is approximately 40% of the perveance limit.

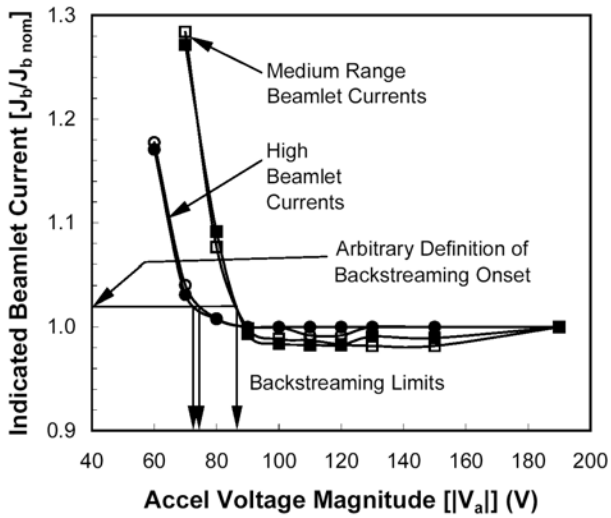

Fig. 9 Typical backstreaming data at medium and high beamlet current values.

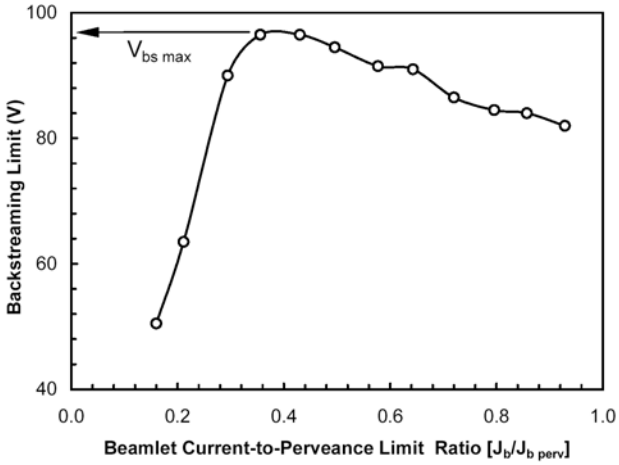

Fig. 10 Backstreaming limit variation as a function of beamlet current.

Backstreaming voltage limits like the ones identified in Figs. 9 and 10 were determined as a function of beamlet current, beam voltage, and grid geometrical changes. The results obtained in this way are plotted in Figs. 11a and 11b for various accel hole diameter and grid spacing conditions. The backstreaming limit for the 60% larger accel hole area condition is larger as expected, but it is difficult to determine a difference between the nominal and the 14% larger diameter hole case. The smaller gapped grid data shown in Fig. 11b display poorer backstreaming behavior compared to the data collected with the larger gapped grid set. The error bars of $\pm$ 5 V on the data points displayed in Figs. 11a and 11b were estimated from the relatively coarse voltage steps used to take the data.

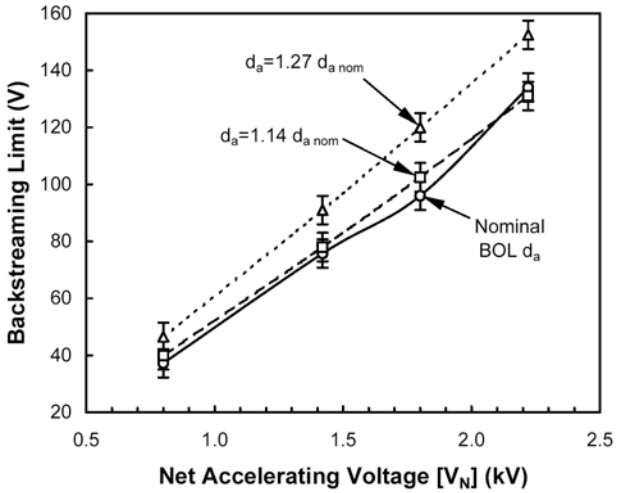

Fig. 11a Effects of accel hole diameter on electron backstreaming.

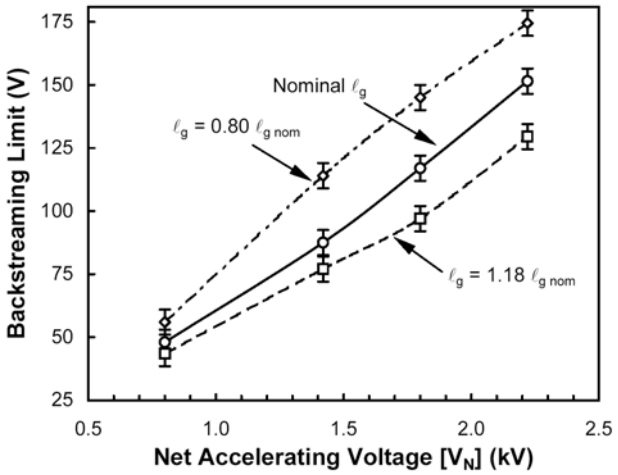

Fig. 11b Effects of grid spacing on electron backstreaming.

Comparison to Numerical Simulation

Figure 12 contains a plot of the perveance limit variation with net accelerating voltage where comparisons are made between experimentally measured limits and numerical simulations. The measurements and simulations were performed at a gridlet spacing that was 9.3% below the nominal CBIO spacing. The numerical simulations were accomplished using the igx code developed by Nakayama and Wilbur.[7] This 3-D code was selected because it can model non-uniform azmuthal variations in beamlet shape that are suspected to give rise to observed beamlet current limitations. The two curves in Fig. 12 show reasonable agreement over a range of net accelerating voltages with better agreement being observed at lower voltages.

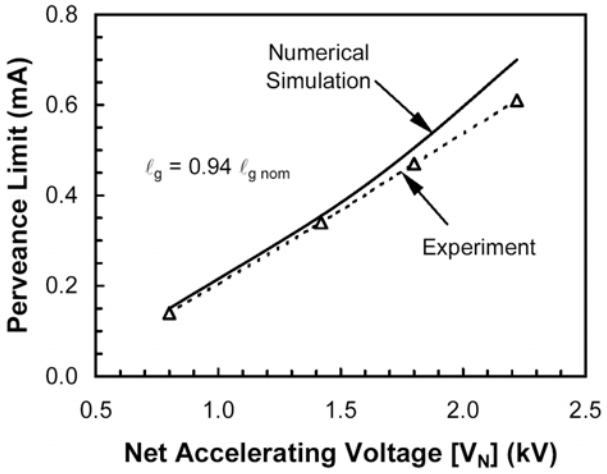

Fig. 12 Comparison between experiment and igx simulation of perveance limit.

The igx code predicts that no crossover ion impingement will occur for the CBIO geometry although crossover is observed in experiments. This same result is obtained when igx is used to simulate the behavior of NSTAR geometry. Close inspection of the numerical results at low beamlet currents suggests that the associated sheaths separating the discharge plasma from the acceleration zone move upstream and flatten as beamlet current is reduced. This causes ions from the discharge plasma to flow uniformly in the axial direction to the screen grid rather than with the radial velocities that give rise to cross over in many grid sets. It is interesting to note that crossover is detected when the igx code is used to simulate SUNSTAR geometries[2] that have dimentions only 50% larger than those for NSTAR.

Figure 13 compares backstreaming limits measured on CBIO gridlets with an accel diameter 27% greater than nominal as a function of net accelerating voltage with corresponding values determined 1) numerically using the igx code[6] and 2) using a recently proposed analytical model[4]. The analytical model, which reflects significant space charge effects, requires the mean beamlet-to-accel hole diameter ratio (d_b/d_a) as input, and values of this ratio were found using the igx code in this case. It is also necessary to input a potential and electron temperature associated with the beam plasma (V_{bp} and T_e, respectively) for the numerical and analytical calculations and 30 V and 1 eV were assumed here to be typical of the experiment. The numerical and analytical approaches are similar in that both yield the accel voltage that must be applied to induce a dip in potential from the beam plasma to a saddle-point minimum along the hole centerline that will stop almost all of the beam electrons from reaching the discharge chamber. In the case of Fig. 13 the acceptable ratio of backstreaming electron to beam ion currents was set at 0.1%.

The numerical and analytical results in the figure are seen to exhibit trends similar to that of the experimental results. Further, the numerical and experimental results match at the 2.22 kV voltage condition and all numerical and analytical results are within about 30 V of the measured values. Finally, it is noted that the beam plasma electron temperature and potential were not measured and different assumptions could be made to bring all of the data into closer agreement.

CONCLUSION

An experimental study of sub-scale **c**arbon-**b**ased **i**on **o**ptics (CBIO) designs proposed by the Jet Propulsion Laboratory (JPL) was performed in which perveance and crossover beamlet current limits were identified over wide throttling ranges. Good agreement is observed between experimental measurements and numerical simulations of perveance limits. Test data collected using grid sets with 1, 7, 19, and 37 apertures suggest that gridlets containing only a small fraction of the total number of apertures in a full-sized optics system can be used to investigate the behavior of larger systems. Evaluations of iso-mica spacers used to insulate gridlets during high power testing indicate that inorganic binder-based iso-mica performs best. Backstreaming voltage limits were measured for different grid spacing to simulate transient behavior and for accel gridlets that were fabricated with progressively larger accel diameters to simulate the effects of accel barrel erosion over life. Analytical and numerical models of electron backstreaming were observed to yield limits that agree reasonably well with experimental values. Based on the ease of conducting the tests and the test data collected to date, we conclude that gridlets can provide a quick and cost-effective method for performing both (1) proof-of-design demonstrations and (2) baseline evaluation of numerical models. The results they provide should also enable performance evaluation of full grid sets that will see radial variations in discharge plasma conditions.

ACKNOWLEDGEMENT

The authors thank JPL for financially supporting this work and Mr.Larry Schwender of Von Roll Isola, Inc., Midwest Mica Division, Cleveland, Ohio, for providing samples of high temperature mica that simplified the task of isolating and spacing the gridlets.

REFERENCES

[1] J.D. Williams, D.M. Laufer, and P.J. Wilbur, "Experimental Performance Limits on High Specific Impulse Ion Optics," IEPC-03-128, International Electric Propulsion Conference, Toulouse France, March 2003.

[2] C.C. Farnell, J.D. Williams, and P.J. Wilbur, "Numerical Simulation of Ion Thruster Optics," 28th International Electric Propulsion Conference, IEPC-03-073, Toulouse, France, 2003.

[3] J.R. Beattie, J.D. Williams, and J.N. Matossian, "Ion Thruster with Long Lifetime Ion Optics System," U.S. Pat. No. 5,924,277, 1999.

[4] J.D. Williams, D.M. Goebel, and P.J. Wilbur, "A Model of Electron Backstreaming in Ion Thrusters," AIAA-2003-4560, 39th Joint Propulsion Conference, Huntsville, AL, 2003.

[5] J.S. Snyder, J.R. Brophy, D.M.Goebel, J.S. Beatty, and M.K. DePano, "Development and Testing of Carbon-Based Ion Optics for 30-cm Ion Thrusters, AIAA-2003- 4716, 39th Joint Propulsion Conference, Huntsville, AL, 2003.

[6] P.J. Wilbur, J. Miller, C.C. Farnell, and V.K. Rawlin, "A Study of High Specific Impulse Ion Thruster Optics," IEPC-01-098, 27th International Electric Propulsion Conference, Pasadena, CA, 2001.

[7] Y. Nakayama and P.J. Wilbur, "Numerical Simulation of High Specific Impulse Ion Thruster Optics, IEPC-01-99, 27th International Electric Propulsion Conference, Pasadena, CA, 2001

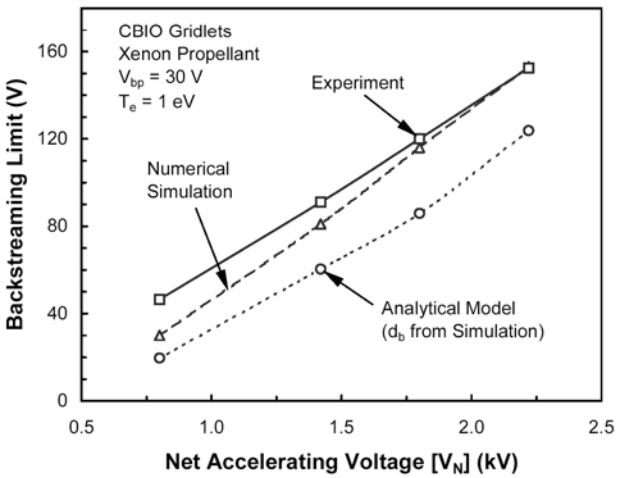

Fig. 13 Comparison between electron backstreaming measurements and simulation results.